Since January 2020 Elsevier has created a COVID-19 resource centre with free information in English and Mandarin on the novel coronavirus COVID-19. The COVID-19 resource centre is hosted on Elsevier Connect, the company's public news and information website.

Veterinary Microbiology 264 (2022) 109299

Contents lists available at ScienceDirect

Veterinary Microbiology

journal homepage: www.elsevier.com/locate/vetmic

Porcine deltacoronavirus infection is inhibited by Griffithsin in cell culture

Rongfeng Tang, Longjun Guo, Qianjin Fan, Liaoyuan Zhang, Yiming Wang, Xin Zhang, Da Shi, Yang Wu, Hongyan Shi, Jianbo Liu, Jianfei Chen *, Li Feng *

Division of Swine Digestive System Infectious Diseases, State Key Laboratory of Veterinary Biotechnology, Harbin Veterinary Research Institute, Chinese Academy of Agricultural Sciences, Harbin 150069, China

ARTICLE INFO

Keywords:
PDCoV
Griffithsin
Lectin
Antiviral activity

ABSTRACT

Porcine deltacoronavirus (PDCoV) is an emerging porcine enteric coronavirus that causes severe diarrhea in piglets and results in serious economic losses. There are no effective vaccines and antiviral drugs to prevent and treat PDCoV infection currently. Griffithsin (GRFT) is a lectin with potent antiviral activity against enveloped viruses because of its ability to specifically bind N-linked high-mannose oligosaccharides. GRFT has been reported to possess antiviral activity against severe acute respiratory syndrome coronavirus (SARS-CoV), Middle East respiratory syndrome coronavirus (MERS-CoV), and porcine epidemic diarrhea virus (PEDV). Here, we first confirmed the antiviral activity of GRFT against PDCoV in vitro. The infected cells (%) and virus titers were significantly decreased at concentration 1 μg/mL or above of GRFT. Time-course experiments revealed that GRFT inhibits PDCoV infection at the adsorption and penetration step. GRFT binding to PDCoV spike (S) protein on the surface wraps the virus and blocks its entry. The outstanding antiviral potency indicates that GRFT has the potential value as a candidate drug for the prevention and treatment of PDCoV infection.

1. Instruction

Coronaviruses are enveloped, positive-sense, single-stranded RNA viruses in the family *Coronaviridae* of the order *Nidovirales* and have the largest RNA genomes among the recognized RNA viruses. Coronaviruses are classified into four groups: *Alphacoronavirus*, *Betacoronavirus*, *Gammacoronavirus* and *Deltacoronavirus*. As an emerging porcine intestinal coronavirus, porcine deltacoronavirus (PDCoV) has been first reported in Hong Kong, China in 2012 (Woo et al., 2012), and later in the USA (Wang et al., 2014), China Mainland (Dong et al., 2015), South Korea (Lee et al., 2016), and Thailand (Lorsirigool et al., 2017). PDCoV can cause severe diarrhea, vomiting, dehydration in piglets (Chen et al., 2015) and serious economic losses in the swine industry. Recently, cases of children infection with PDCoV have been reported in Haiti (Lednicky et al., 2021).

Lectins are proteins that bind to specific carbohydrate structures. Griffithsin (GRFT), a high-mannose-specific lectin isolated from marine red algae (*Griffithsia* sp.), exists as a homodimer with three carbohydrate-binding domains (CBDs) per monomer and has broad-spectrum antiviral activity. GRFT exerts antiviral activity against multiple coronaviruses, including severe acute respiratory syndrome coronavirus (SARS-CoV) (O'Keefe et al., 2010), Middle East respiratory syndrome coronavirus (MERS-CoV) (Millet et al., 2016), feline coronavirus (FCoV) (Hsieh et al., 2010), and porcine epidemic diarrhea virus (PEDV) (Li et al., 2019). Moreover, researches on GRFT against human immunodeficiency virus (HIV) have been deep and extensive for decades (Akkouh et al., 2015; Lee, 2019). GRFT carrageenan fast-dissolving inserts were reported to protect rhesus macaques from HIV and human papillomavirus (HPV) vaginal challenge and showed the potential for clinical application (Derby et al., 2018).

In this study, we assessed the antiviral activity of GRFT against PDCoV in IPI-2I cells, further identified the role of GRFT in the viral replication cycle and elucidated the detailed mechanism of GRFT inhibitory action on PDCoV infection.

2. Materials and methods

2.1. Cells and virus

Swine testis (ST) cells, porcine intestinal epithelial (IPI-2I) cells, human embryonic kidney (293T) cells were grown in Dulbecco's Modified Eagle Medium (DMEM) (Gibco, USA), supplemented with 10 % FBS (Gibco, USA). The cells were grown at 37℃ in a 5% CO_2 incubator. PDCoV strain NH passage 10 (P10) was grown and titrated in ST

* Corresponding authors.
E-mail addresses: chenjianfei@caas.cn (J. Chen), fengli@caas.cn (L. Feng).

https://doi.org/10.1016/j.vetmic.2021.109299
Received 8 August 2021; Received in revised form 23 November 2021; Accepted 5 December 2021
Available online 7 December 2021

cells (Zhang et al., 2019).

2.2. GRFT expression and purification

The codon-optimized gene encoding GRFT (GenBank: FJ594069) was synthesized by BGI Genomics in China and cloned into the pET24b (+) vector (Novagen, Germany) to be in frame with a 6×His-tag. Then the plasmid transformed into competent cells BL21 (Takara, China). The protein expression was induced with IPTG at a final concentration of 1 mM at 16℃ for ten hours. The bacteria cells were harvested, resuspended and further lysed with pulsed sonication on ice. GRFT in the cleared lysate was purified by His60 Ni Superflow Resin (Takara, China) according to manufacturer's guidelines. Finally, the purified protein was analyzed by SDS-PAGE and western blot.

2.3. Cell viability assay

Cytotoxicity was evaluated using a Cell Counting Kit-8 (DOJINDO, Japan). ST cells and IPI-2I cells were seeded in wells of a 96-well plate at a density of 2×10^4 cells per well. The next day, cells were treated with several doses of GRFT, or with an equal volume of DMEM serving as a negative control and cell-free DMEM serving as a background. After incubating for 24 h, cells were added with CCK-8 and incubated for an additional 2 h at 37℃, then measured the absorbance at 450 nm. The percent cell viability was calculated by the following equation:

$$\text{Cell viability}(\%) = \frac{A_{450}(\text{Cells with GRFT}) - A_{450}(\text{Background})}{A_{450}(\text{Negative control}) - A_{450}(\text{Background})}\%$$

The inhibition rates (%) of GRFT against PDCoV infection on ST cells and IPI-2I cells were also measured by CCK-8. The cells were infected with PDCoV at a multiplicity of infection (MOI) of 1 while various doses of GRFT were added. Non-infected cells and DMEM-treated virus inoculum were used as negative controls. At 24 h post infection (hpi), CCK-8 was added to determine cell viability. The inhibition rate of lectin was calculated by the following equation:

$$\text{Inhibition rate}(\%) = \frac{A_{450}(\text{GRFT} - \text{treated}) - A_{450}(\text{DMEM} - \text{treated})}{A_{450}(\text{Non} - \text{infected}) - A_{450}(\text{DMEM} - \text{treated})}\%$$

Regression analysis of the cell viability (%) data and the inhibition rate (%) data yielded the 50 % cytotoxic dose (CC_{50}) and 50 % effective dose (EC_{50}), respectively. The therapeutic index (SI) was computed using the formula: $SI = EC_{50}/CC_{50}$ for distinct cells.

2.4. Immunofluorescence assay

2.5×10^5 IPI-2I cells seeded in 24-well plates for 24 h. PDCoV NH P10 was pre-incubated with 10, 1, 0.1, 0.01, 0 μg/mL GRFT for 2 h at 37℃, then infected the cells. Non-infected cells were served as a negative control. At 24 hpi, the cells were fixed with 4% paraformaldehyde, permeabilized with 0.1 % (w/v) Triton X-100, and blocked with 5% (w/v) skimmed milk. Then, the cells were incubated with anti-PDCoV-N mouse monoclonal antibody (Su et al., 2016) for 1 h at 37℃, after washed with PBS and stained with donkey anti-mouse lgG(H + L) antibody (Invitrogen, USA) for 40 min at 37℃, followed by DAPI nuclear staining. The cells were counted by Image J and infected cells (%) were calculated by GFP cells/DAPI cells.

2.5. Effect of GRFT on viral production

1.0×10^6 IPI-2I cells were seeded in 6-well plates for 24 h. The methods of virus infection and GRFT administration were described above. At 18 hpi, cell pellets were harvested and stored at -20℃. To identify the expression of PDCoV nucleocapsid (N) protein, cell pellets were lysed by RIPA (Sigma, USA) for 30 min at room temperature and then detected with an anti-PDCoV-N mouse monoclonal antibody. Gray value was analyzed using Image J.

Viral RNA was extracted by RNAiso Plus (Takara) from cell pellets, and cDNA was synthesized by PrimeScript IV 1st strand cDNA Synthesis Mix (Takara, China). The forward primer and reverse primer for PDCoV N and β-actin were as follows: PDCoV-N-F, 5′- AGCAACCACTCGTGTTACTTG-3′; PDCoV-N-R, 5′-CAACTCTGAAACCTTGAGCTG-3′; β-actin-F, 5′-CTTCCTGGGCATGGAGTCC-3′; β-actin-R: 5′-GGCGCGATGATCTTGATCTTC-3′. RT-qPCR was performed with the TB Green Premix Ex Taq II (Takara, China). Data were analyzed using the $2^{-\Delta\Delta Ct}$ method.

2.6. Effect of GRFT on viral entry steps

2.5×10^5 IPI-2I cells seeded in 24-well plates for 24–28 h. GRFT was added in five different stages: (1) virus at a MOI = 1 attached to the pre-cooled cells for 1 h at 4℃, (2) DMEM washed to remove unbound virus, further binding for 1 h at 4℃, (3) internalization for 1 h at 37℃, (4) 1 h post internalization at 37℃, (5) 2 h post internalization at 37℃. After 24 hpi, the cells were fixed and processed for immunofluorescence assay as described previously.

2.7. Mannose competitive inhibition

GRFT at 1 μg/mL was either pre-incubated with 1 M G-(+)-Mannose (Sigma, USA) for 1 h at 37℃ or not. The cells were infected with PDCoV NH P10 of MOI = 1 and then placed in DMEM, mannose pre-incubated GRFT, and GRFT. Cultured for 36 h, the supernatant was harvested for $TCID_{50}$ assay, and viral RNA was extracted from lysed cells and quantified the relative amount of N mRNA by RT-qPCR as previously mentioned.

2.8. Interaction of GRFT and PDCoV spike protein

PDCoV virions were treated with 1 μg/mL GRFT or DMEM for 1 h at 37℃. Virus particles were observed by electron microscopy.

The interaction between GRFT and PDCoV spike (S) protein was verified by ELISA. Purified S, S1, and S2 protein were immobilized to a 96-well plate (50 ng per well) by incubation at 4℃ overnight and blocked with 5% skimmed milk at 37℃ for 2 h. After washed with PBS, the wells were incubated with $\log_{10}$ serial dilutions of GRFT for 2 h at 37℃. The plates were washed and incubated with HRP-conjugated rabbit anti-6×His-tag polyclonal antibodies (Abcam, UK) for 1 h at 37℃. After incubated with 3,3′,5,5′-Tetramethylbenzidine (Sigma, USA) for 10 min, the reactions were stopped by the addition of 2 M H_2SO_4, and the absorbance was measured at 450 nm.

2.9. Statistical analyses

Analysis of experimental data, calculations of standard deviations (s.d.) and graph plotting were performed using GraphPad Prism 7.0. Statistical analyses were performed using Nonlinear regression (dose-response for cell viability and viral infection) and two-tailed Student's *t*-test (virus titer assays, competition with Mannose and RT-qPCR assay). For *p*-value significance, the following convention was used: not significant (n.s.) $p > 0.05$, significant (*) $p \leq 0.05$, highly significant (**) $p \leq 0.01$, very highly significant (***) $p \leq 0.001$.

3. Results

3.1. Expression and purification of GRFT

Purified GRFT was identified by SDS-PAGE (Fig. 1A) and western blot (Fig. 1B) using mouse anti-His monoclonal antibody (Abcam, UK). The results showed that GRFT was successfully expressed and purified, and its molecular weight was about 15 kD. The purified protein was dialyzed, following by filter sterilization prior to use.

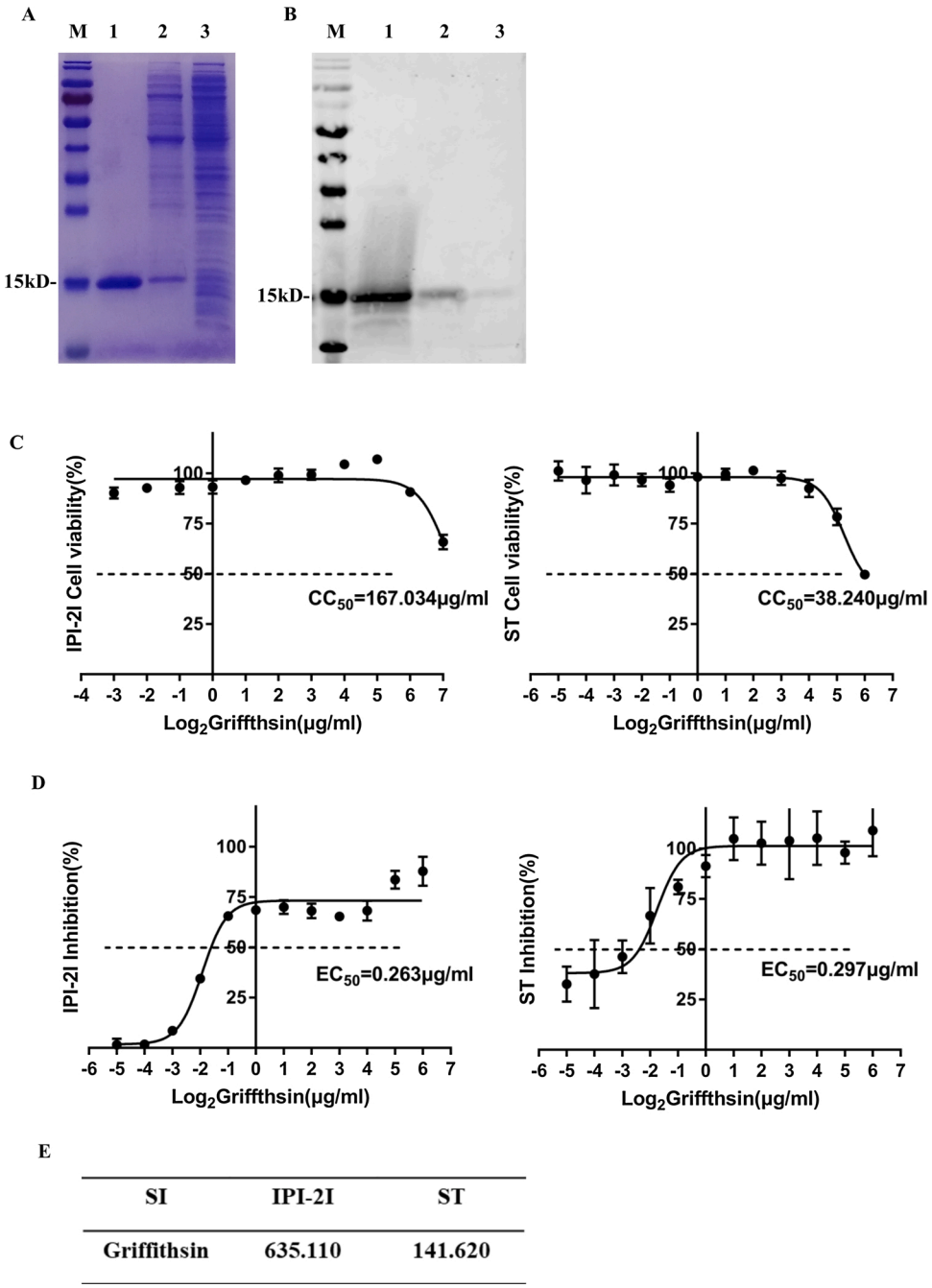

Fig. 1. Purification, effect of GRFT on cells viability and PDCoV infectivity. (A-B) SDS-PAGE and western blot analysis of purified GRFT. Lane M protein size markers, Lane 1 elution of GRFT, Lane 2 wash buffer through the resin, Lane 3 supernatant of lysed suspension. The molecular weight is about 15 kD. (C) ST and IPI-2I cell viability after 24 h incubation with different concentrations of GRFT by CCK-8 Kit. CC_{50} (50 % cytotoxic dose) was figured by cell viability (%). (D) ST and IPI-2I cell viability after 24 h incubation with different concentrations of GRFT and PDCoV at MOI = 1. EC_{50} (50 % effective dose) was figured by inhibition rate (%). (E) The therapeutic index (SI) was figured by CC_{50}/EC_{50}. The SI showed GRFT had good safety and anti-infection activity.

E

SI	IPI-2I	ST
Griffithsin	635.110	141.620

3.2. Dose-response inhibition of GRFT on PDCoV infection

The cytotoxic of GRFT on cell viability was assessed by treating ST cells and IPI-2I cells with a range of GRFT concentrations from 2^{-6} to 2^{6} μg/mL. As illustrated in Fig. 1C, GRFT showed minimal cytotoxicity to IPI-2I and ST cells (IPI-2I CC_{50} = 167.034 μg/mL, ST CC_{50} = 38.240 μg/mL). Based on its security range, the inhibition rate of GRFT against PDCoV infection was calculated with the cell viability, the values of EC_{50} on IPI-2I cells and ST cells were 0.263 μg/mL and 0.297 μg/mL, respectively (Fig. 1D). Therapeutic indexes on IPI-2I and ST cells reached 635.11 and 141.62 (Fig. 1E) respectively, indicating that GRFT was safe and effective against PDCoV.

Immunofluorescence assay revealed that GRFT inhibited PDCoV infection on IPI-2I cells (Fig. 2A), with the increase of GRFT concentration, the cell infection rate declined gradually from 20.92 % to 0.077 % (Fig. 2B). There was a marked declined trend on the expression of PDCoV N protein with the increase of GRFT doses detected by western-blot (Fig. 2C) accompanied by gray value analysis (Fig. 2D), and the same trend occurred on the relative PDCoV N mRNA level determined by RT-qPCR (Fig. 2E). All the results showed that the antiviral effect was highly significant above a dose of 1 μg/mL ($p \leq 0.001$).

To investigate the effect of GRFT on PDCoV production, IPI-2I cells were infected with PDCoV in the presence or not of 1 μg/mL GRFT. $TCID_{50}$ assay showed that virus titers significantly decreased from $10^{4.38}$ to $10^{1.25}$ $TCID_{50}$/mL after GRFT treatment ($p < 0.05$) (Fig. 2F).

3.3. Mannose competitive inhibition the effect of GRFT

A mannose competition assay was performed to confirm that the inhibition observed was unique to the characteristics of GRFT. In $TCID_{50}$

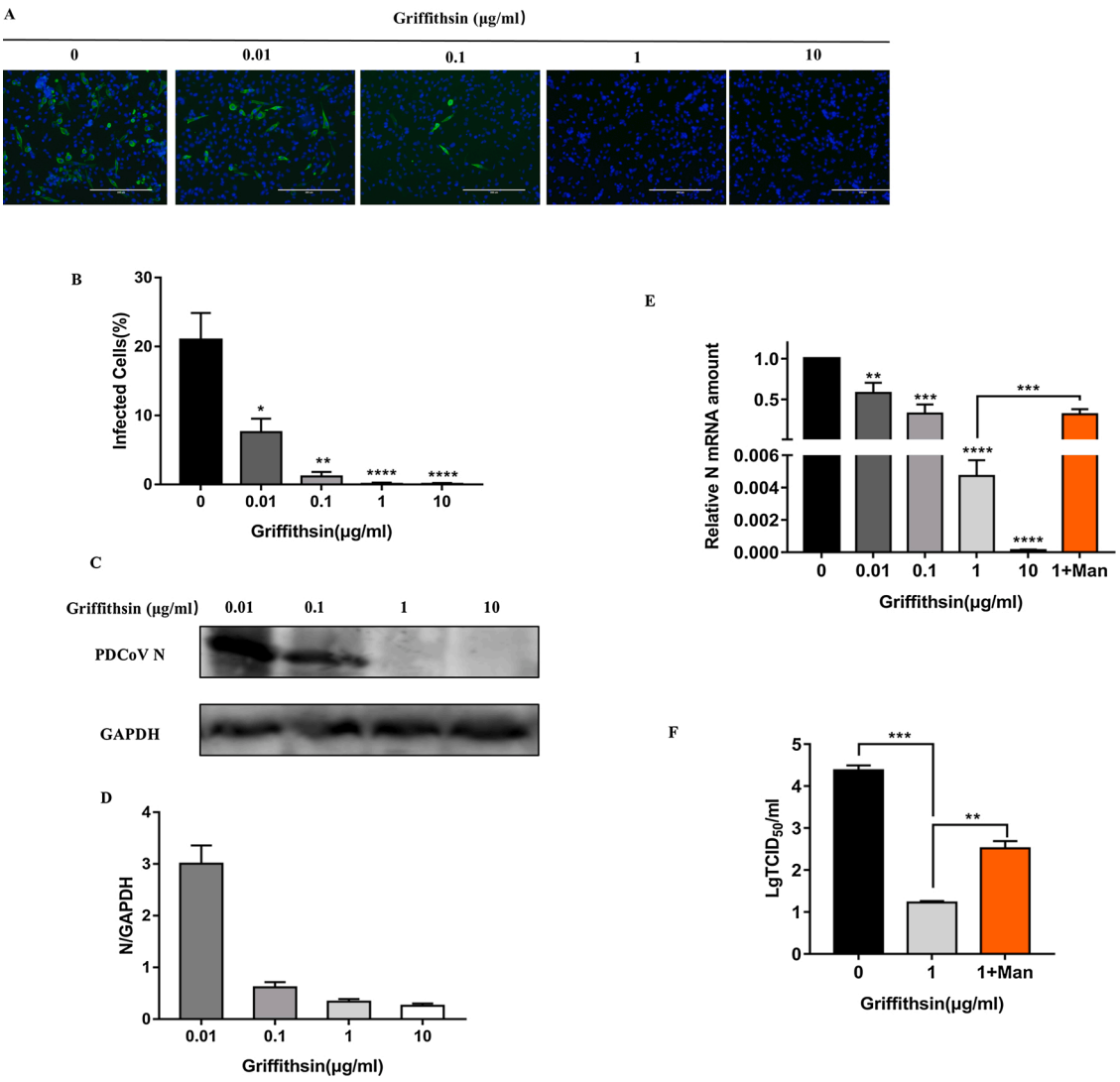

Fig. 2. Dose-response of GRFT inhibition against PDCoV infection and mannose competitive inhibition. (A) Immunofluorescence assay of PDCoV-infected IPI-2I cells in presence of increasing concentrations of GRFT. (B) For each condition, three 20× objective fields were randomly acquired and analyzed for a total number of cells (DAPI nuclei stain) and N-positive cells (infected cells). Results are expressed as percentage infected cells. (C) Western-blot assay of PDCoV N protein. (D) A gray value analysis of western-blot result. (E) Relative N mRNA amount was measured by RT-qPCR. The results showed that GRFT had a remarkable inhibition against PDCoV infection at concentrations above 1 μg/mL. The orange column indicated that relative N mRNA level rose after mannose treatment. (F) Virus titers decreased markedly with treatment of 1 μg/mL GRFT at the infection process. However, pre-incubation of GRFT with mannose could significantly antagonize the antiviral effect of GRFT and increase the virus titer.

assay, compared with not pre-incubated GRFT, the virus titer of GRFT pre-incubated with mannose group rose markedly from $10^{1.25}$ to $10^{2.52}$ $TCID_{50}$/mL, but it still retained antiviral effect compared with DMEM positive control. The relative N mRNA level was increased about 67 times after treatment of mannose ($p \leq 0.001$) (Fig. 2E), showing that mannose could antagonize GRFT's antiviral activity.

3.4. GRFT acts on viral entry stages

To define which stage in the virus life cycle GRFT played role in, IPI-2I cells were infected by PDCoV with GRFT 1 μg/mL present at different points during viral entrance steps (Fig. 3A). Viral entry steps were divided into attachment at 4℃, binding at 4℃, internalization at 37℃. GRFT was also added 1 hpi and 2 hpi to see if it affected the internalized virus. Immunofluorescence observations illustrated GRFT is primarily involved in the attachment stage and has effects on viruses that have been bind on the cell surface and their internalization process, nevertheless, GRFT is little effective for viruses that have been internalized into the cell. Infectivity decreased significantly from 24.73 % to 0.08 %, 0.51 % and 0.65 % in conditions (b), (c) and (d), respectively (Fig. 3C), while conditions (c) and (d) had slightly more infected cells than condition (b) (Fig. 3B), revealing that GRFT might focus on the attachment stage. However, after virus internalization, the infected rates of conditions (e) and (f) rose to 5.09 % and 10.12 % indicating that GRFT could not effectively prevent cell infection from internalized PDCoV and that the later GRFT was added, the weaker the antiviral activity was (Fig. 3C).

3.5. Binding ability of GRFT with S and its subunits

The untreated PDCoV presented a typical coronavirus pattern (Fig. 4A). PDCoV virions were surrounded with floccule when treated by 1 μg/mL GRFT, and the viral spike was no longer visible (Fig. 4B).

To further confirm interactions between GRFT with PDCoV S protein and its subunits, ELISA assays were performed. As shown in Fig. 4C, with the increase of GRFT concentration, the absorbance value (OD_{450}) also

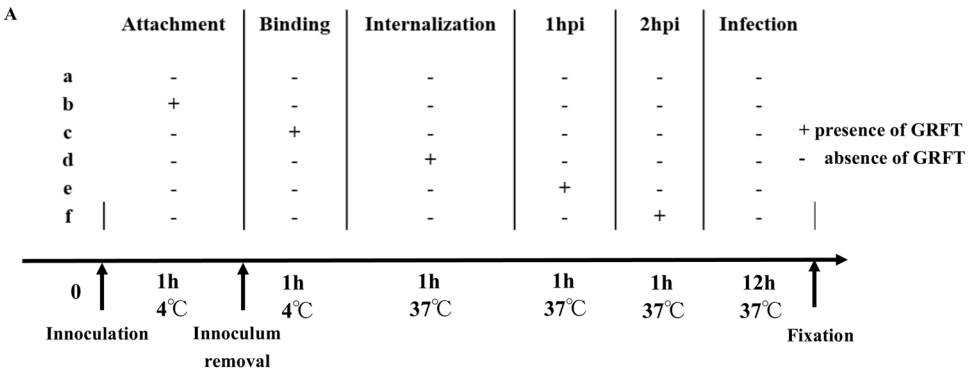

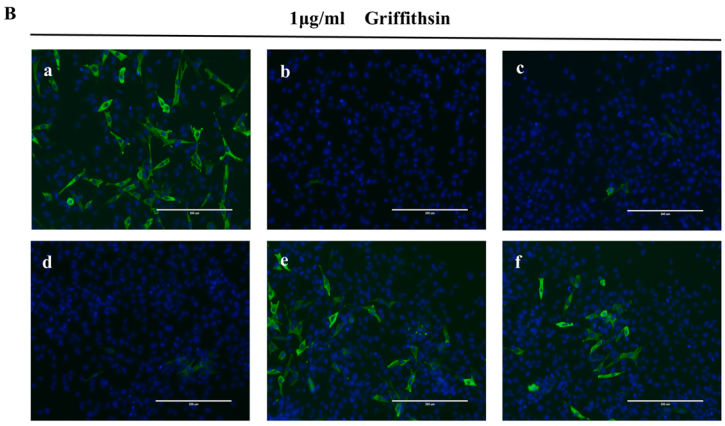

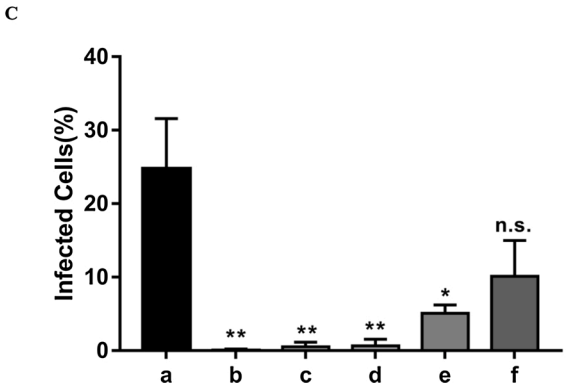

Fig. 3. Antiviral activity of GRFT at initial stages of PDCoV infection. (A) Schematic of the additional time course. GRFT was administered at different stages of PDCoV infection including (b) attachment at 4℃, (c) further binding at 4℃, (d) internalization at 37℃, (e) 1 hpi, and (f) 2 hpi, each step lasted for 1 h. (B) Immunofluorescence assay of PDCoV infected IPI-2I cells with GRFT present at different stages of infection. (C) Infected cells (%) was analysed by Image J. Infected cells (%) of conditions (b), (c) and (d) significantly decreased ($p < 0.05$), conditions (e) and (f) were not significantly different with condition (a) without medication ($p > 0.05$).

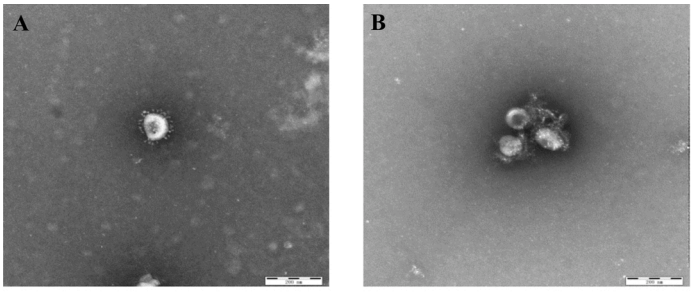

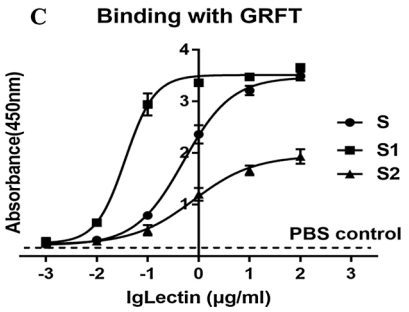

Fig. 4. Interaction between GRFT and PDCoV S protein. (A) Untreated PDCoV virus particles (B) After being treated by 1 μg/mL GRFT, PDCoV virus particles were wrapped in a floccule. Through the interaction of GRFT and S protein, viruses were encapsulated and the spikes of PDCoV were sealed, thus preventing virus entry. (C) GRFT binds directly to PDCoV S protein (●), S1 protein (■), and S2 protein (▲). PBS control was indicated by the dotted line. The combination ability of GRFT with S1, S, S2 is from strong to weak.

increased and reached 3.385 in S, 3.677 in S1 and 1.931 in S2, respectively (Fig. 4C). GRFT has stronger binding ability with S1 compared to S2, which might depend not only on the glycosylation of S1 and S2 subunits, but also on the modification of mannose.

4. Discussion

In recent years, particularly with the outbreak of COVID-19, there have been increasing researches on antiviral medications against coronaviruses. Various molecular compounds against PDCoV in vitro and in vivo through different pathways were reported successively including Remdesivir (Brown et al., 2019), ergosterol peroxide (Duan et al., 2021), bile acids (Kong et al., 2021) for the past several years. Until now, there have been no clinical records of effective antiviral drugs for the treatment of infection. Therefore, medication discovery for the prevention and treatment of PDCoV infection remains critical and urgent. GRFT, as a potential broad-spectrum antiviral drug, has high application value but its antiviral effect on PDCoV is unknown.

In this study, we provided evidences that GRFT exhibits antiviral activity against PDCoV and security in vitro. Moreover, we explained the basic mechanism of GRFT function in viral entrance through its interaction with S protein. GRFT may be a promising tool in the prevention and treatment of PDCoV infection.

The effective concentration of GRFT against PDCoV at MOI = 1 was 1 μg/mL according to our results. Immunofluorescence, western-blot, and RT-qPCR data indicated that the infected cells (%), grayscale value, and relative N mRNA level were significantly decreased respectively ($p < 0.0001$) when GRFT concentration was 1 μg/mL or higher. GRFT also displayed antiviral activity against other coronaviruses at similar dosages including SARS-CoV (O'Keefe et al., 2010), MERS-CoV (Millet et al., 2016), PEDV (Li et al., 2019). The concentration of GRFT against HCV was comparable to that of coronaviruses (Meuleman et al., 2011). However, the effective concentration of GRFT against other enveloped viruses varies greatly. GRFT can be used to prevent HIV infection at a low concentration of 1 mM (Lee, 2019), while the effective concentration against Hantavirus infection is higher, reaching more than 25 μg/mL (Shrivastava-Ranjan et al., 2020). This diversity may be attributed to different degrees of glycosylation of each viral membrane protein and densities of glycosylated protein.

As a novel coronavirus, the structure and function of the PDCoV S protein is semblable to the other coronaviruses. PDCoV S protein is highly glycosylated and divided into S1 and S2 domains, which is major determinants of virus entry and tropism. The S1 domain is responsible for receptor binding and viral attachment to the host cell surface, whereas S2 contains the fusion machinery. We demonstrated that GRFT can bind to S, S1, and S2 proteins and the binding capacity of S1 and S2 subunits are related to the degree of glycosylation of the subunits. The reports of Cryo-Electron microscopy structure of PDCoV S protein suggested that both S1 and S2 had abundant glycosylation sites (Shang et al., 2018), and above half of the glycosylation sites were highly mannose modified (Xiong et al., 2018). Meanwhile, based on the analytical and predicted glycosylation sites, S1 has more glycosylation sites than S2, and 11 of 15 glycosylation sites in S1 have mannose modification, while only 5 of 11 glycosylation sites in S2 have mannose modification. These observations further prove that GRFT plays a role in the virus entry stage, with a stronger role in the attachment step. Mannose can also prevent the antiviral effect of GRFT by antagonizing the GRFT interaction with S protein. The molecular mechanism of the GRFT antiviral effect is revealed preliminary.

We found that GRFT plays a role in both viral adsorption and internalization, but the effect was slightly stronger in the adsorption stage. Barry R. O'Keefe and his colleagues found that GRFT could not prevent the SARS-CoV S from binding with cellular receptor ACE2, suggesting that GRFT may block subsequent steps for viral entry (O'Keefe et al., 2010). For MERS-CoV, GRFT works only in the viral attachment phase, likely by preventing interaction between S protein and DPP4 (Millet et al., 2016). The discrepancy might be related to differences in viral receptors and the viral invasion process. Unfortunately, the PDCoV receptor has yet been defined (Belouzard et al., 2012). However, the current consensus is that GRFT works only during the virus entry phase, but is useless when the virus has already entered the cells.

5. Conclusion

In conclusion, we confirmed that GRFT has anti-PDCoV activity by inhibition of viral attachment and internalization. GRFT prevents virus invasion by interacting with PDCoV S protein. Based on these characteristics, GRFT may be utilized to prevent and treat PDCoV and other porcine enteric coronaviruses.

Author contribution

Conception, R.T., J.C. and L.F.; methodology, R.T., L.G., Q.F., L.Z., Y. W.; manuscript writing, R.T. and J.C.; constructive discussion, X.Z., Y.W. and H.S.; supervision, D.S. J.L. and L.F. All authors have read and agreed to the published version of the manuscript.

Declaration of Competing Interest

The authors declare that they have no conflict of interest.

Acknowledgments

This study was supported by grants from the Natural Science Foundation of Heilongjiang province of China (TD2020C002), Heilongjiang province for Major Program of National science and technology and the National Key Research and Development Program of China (GX18B008) and Project of State Key Laboratory of Veterinary Biotechnology (SKLVBP202105).

References

Akkouh, O., Ng, T.B., Singh, S.S., Yin, C., Dan, X., Chan, Y.S., Pan, W., Cheung, R.C., 2015. Lectins with anti-HIV activity: a review. Molecules (Basel, Switzerland) 20, 648–668.

Belouzard, S., Millet, J.K., Licitra, B.N., Whittaker, G.R., 2012. Mechanisms of coronavirus cell entry mediated by the viral spike protein. Viruses 4, 1011–1033.

Brown, A.J., Won, J.J., Graham, R.L., Dinnon 3rd, K.H., Sims, A.C., Feng, J.Y., Cihlar, T., Denison, M.R., Baric, R.S., Sheahan, T.P., 2019. Broad spectrum antiviral remdesivir inhibits human endemic and zoonotic deltacoronaviruses with a highly divergent RNA dependent RNA polymerase. Antiviral Res. 169, 104541.

Chen, Q., Gauger, P., Stafne, M., Thomas, J., Arruda, P., Burrough, E., Madson, D., Brodie, J., Magstadt, D., Derscheid, R., Welch, M., Zhang, J., 2015. Pathogenicity and pathogenesis of a United States porcine deltacoronavirus cell culture isolate in 5-day-old neonatal piglets. Virology 482, 51–59.

Derby, N., Lal, M., Aravantinou, M., Kizima, L., Barnable, P., Rodriguez, A., Lai, M., Wesenberg, A., Ugaonkar, S., Levendosky, K., Mizenina, O., Kleinbeck, K., Lifson, J. D., Peet, M.M., Lloyd, Z., Benson, M., Heneine, W., O'Keefe, B.R., Robbiani, M., Martinelli, E., Grasperge, B., Blanchard, J., Gettie, A., Teleshova, N., Fernández-Romero, J.A., Zydowsky, T.M., 2018. Griffithsin carrageenan fast dissolving inserts prevent SHIV HSV-2 and HPV infections in vivo. Nat. Commun. 9, 3881.

Dong, N., Fang, L., Zeng, S., Sun, Q., Chen, H., Xiao, S., 2015. Porcine deltacoronavirus in Mainland China. Emerging Infect. Dis. 21, 2254–2255.

Duan, C., Wang, J., Liu, Y., Zhang, J., Si, J., Hao, Z., Wang, J., 2021. Antiviral effects of ergosterol peroxide in a pig model of porcine deltacoronavirus (PDCoV) infection involves modulation of apoptosis and tight junction in the small intestine. Vet. Res. 52, 86.

Hsieh, L.E., Lin, C.N., Su, B.L., Jan, T.R., Chen, C.M., Wang, C.H., Lin, D.S., Lin, C.T., Chueh, L.L., 2010. Synergistic antiviral effect of Galanthus nivalis agglutinin and nelfinavir against feline coronavirus. Antiviral Res. 88, 25–30.

Kong, F., Niu, X., Liu, M., Wang, Q., 2021. Bile acids LCA and CDCA inhibited porcine deltacoronavirus replication in vitro. Vet. Microbiol. 257, 109097.

Lednicky, J.A., Tagliamonte, M.S., White, S.K., Elbadry, M.A., Alam, M.M., Stephenson, C.J., Bonny, T.S., Loeb, J.C., Telisma, T., Chavannes, S., Ostrov, D.A., Mavian, C., Beau De Rochars, V.M., Salemi, M., Morris, J.G., 2021. Independent infections of porcine deltacoronavirus among Haitian children. Nature. https://doi.org/10.1038/s41586-021-04111-z.

Lee, C., 2019. Griffithsin, a highly potent broad-spectrum antiviral lectin from red algae: from discovery to clinical application. Mar. Drugs 17.

Lee, J.H., Chung, H.C., Nguyen, V.G., Moon, H.J., Kim, H.K., Park, S.J., Lee, C.H., Lee, G. E., Park, B.K., 2016. Detection and phylogenetic analysis of porcine deltacoronavirus in Korean swine farms, 2015. Transbound. Emerg. Dis. 63, 248–252.

Li, L., Yu, X., Zhang, H., Cheng, H., Hou, L., Zheng, Q., Hou, J., 2019. In vitro antiviral activity of Griffithsin against porcine epidemic diarrhea virus. Virus Genes 55, 174–181.

Lorsirigool, A., Saeng-Chuto, K., Madapong, A., Temeeyasen, G., Tripipat, T., Kaewprommal, P., Tantituvanont, A., Piriyapongsa, J., Nilubol, D., 2017. The genetic diversity and complete genome analysis of two novel porcine deltacoronavirus isolates in Thailand in 2015. Virus Genes 53, 240–248.

Meuleman, P., Albecka, A., Belouzard, S., Vercauteren, K., Verhoye, L., Wychowski, C., Leroux-Roels, G., Palmer, K.E., Dubuisson, J., 2011. Griffithsin has antiviral activity against hepatitis C virus. Antimicrob. Agents Chemother. 55, 5159–5167.

Millet, J.K., Séron, K., Labitt, R.N., Danneels, A., Palmer, K.E., Whittaker, G.R., Dubuisson, J., Belouzard, S., 2016. Middle East respiratory syndrome coronavirus infection is inhibited by griffithsin. Antiviral Res. 133, 1–8.

O'Keefe, B.R., Giomarelli, B., Barnard, D.L., Shenoy, S.R., Chan, P.K., McMahon, J.B., Palmer, K.E., Barnett, B.W., Meyerholz, D.K., Wohlford-Lenane, C.L., McCray Jr., P. B., 2010. Broad-spectrum in vitro activity and in vivo efficacy of the antiviral protein griffithsin against emerging viruses of the family Coronaviridae. J. Virol. 84, 2511–2521.

Shang, J., Zheng, Y., Yang, Y., Liu, C., Geng, Q., Tai, W., Du, L., Zhou, Y., Zhang, W., Li, F., 2018. Cryo-electron microscopy structure of porcine deltacoronavirus spike protein in the prefusion state. J. Virol. 92.

Shrivastava-Ranjan, P., Lo, M.K., Chatterjee, P., Flint, M., Nichol, S.T., Montgomery, J. M., O'Keefe, B.R., Spiropoulou, C.F., 2020. Hantavirus infection is inhibited by griffithsin in cell culture. Front. Cell. Infect. Microbiol. 10, 561502.

Su, M., Li, C., Guo, D., Wei, S., Wang, X., Geng, Y., Yao, S., Gao, J., Wang, E., Zhao, X., Wang, Z., Wang, J., Wu, R., Feng, L., Sun, D., 2016. A recombinant nucleocapsid protein-based indirect enzyme-linked immunosorbent assay to detect antibodies against porcine deltacoronavirus. J. Vet. Med. Sci. 78, 601–606.

Wang, L., Byrum, B., Zhang, Y., 2014. Detection and genetic characterization of deltacoronavirus in pigs, Ohio, USA, 2014. Emerging Infect. Dis. 20, 1227–1230.

Woo, P.C., Lau, S.K., Lam, C.S., Lau, C.C., Tsang, A.K., Lau, J.H., Bai, R., Teng, J.L., Tsang, C.C., Wang, M., Zheng, B.J., Chan, K.H., Yuen, K.Y., 2012. Discovery of seven novel Mammalian and avian coronaviruses in the genus deltacoronavirus supports bat coronaviruses as the gene source of alphacoronavirus and betacoronavirus and avian coronaviruses as the gene source of gammacoronavirus and deltacoronavirus. J. Virol. 86, 3995–4008.

Xiong, X., Tortorici, M.A., Snijder, J., Yoshioka, C., Walls, A.C., Li, W., McGuire, A.T., Rey, F.A., Bosch, B.J., Veesler, D., 2018. Glycan shield and fusion activation of a deltacoronavirus spike glycoprotein fine-tuned for enteric infections. J. Virol. 92.

Zhang, J., Chen, J., Shi, D., Shi, H., Zhang, X., Liu, J., Cao, L., Zhu, X., Liu, Y., Wang, X., Ji, Z., Feng, L., 2019. Porcine deltacoronavirus enters cells via two pathways: a protease-mediated one at the cell surface and another facilitated by cathepsins in the endosome. J. Biol. Chem. 294, 9830–9843.